SYNTHETIC LINE PROFILES FROM NUMERICAL SIMULATIONS OF A RED SUPERGIANT

Bernd Freytag[1,2], Michelle Mizuno-Wiedner[2], Bengt Gustafsson[2]

[1]GRAAL, Université de Montpellier II, France
[2]Department for Astronomy and Space Physics at Uppsala University, Sweden

Abstract

Radiation hydrodynamics simulations of the outer envelope and atmosphere of a red supergiant have been performed with CO^{5}BOLD. In this poster we demonstrate the relation between the local temperature and velocity stratifications and the (spatially and temporally resolved) intensity line profiles calculated from them. Furthermore, we discuss the temporal variations of the flux profiles and compare with observations by David Gray.

Key words: convection, hydrodynamics, radiative transfer, spectrum synthesis, methods: numerical, stars: atmospheres, stars: red supergiants

1. Models and synthetic spectra of Betelgeuse

The CO^{5}BOLD code has been used to model the outer layers of the red supergiant Betelgeuse (M1-2 Ia-Iab). The code numerically integrates the coupled non-linear equations of compressible hydrodynamics and non-local radiation transport on a Cartesian grid, and accounts for ionization effects and realistic (grey) opacities. Gravitation is represented as a spherical $1/r$ potential, smoothed in the center.

The parameters of Betelgeuse (M1-2 Ia-Iab) are not very well known ($R = 600 - 1000\,R_\odot$, $M = 5 - 20\,M_\odot$, $T_{\rm eff} = 3400 - 3600\,$K). The parameters for the model `st35gm04n29` presented here ($T_{\rm eff} \sim 3330\,$K, $R_\star \sim 630\,R_\odot$, $\log g \sim -0.46$ in cgs units, $L_\star \sim 42\,000\,L_\odot$, and especially the rather low mass $M_\star = 5 M_\odot$) were chosen to favor large convective cells to make it easier to resolve them on a given numerical grid—in this case a cube with 235^3 grid points and edge length $1626\,R_\odot$. Post-processing consisted of spectrum synthesis for a single Fe I line (λ=6219.281 Å, excitation energy 2.198 eV), for 67 snapshots covering a simulation time of 4.2 years.

2. Observations

The irregular light curve of Betelgeuse (Goldberg 1984), interferometric detections of hot-spots in the optical (e.g., Buscher et al. 1990; Burns et al. 1997, Young et al. 2000), and inhomogeneities in the atmosphere (observed by Lim et al. 1998, with the VLA) or chromosphere (Gilliland & Dupree 1996 with the HST) favor a picture of the near-surface layers with large-scale structures and violent motions. From simple scaling arguments, Schwarzschild (1975) suggested that a few giant convective cells on the surface of Betelgeuse are the cause for the observed temporal brightness variations. This is also what is proposed by the 3D radiation hydrodynamics simulations of Freytag, whose models reveal a variety of surface features that can be attributed to small surface and large envelope convection cells, to pressure fluctuations in the stellar interior, and to shock waves in the atmosphere (see, e.g., Freytag et al. 2002). However, Gray (2000, 2001) has argued that the stability of photospheric line profiles in the spectrum of Betelgeuse suggests that the stellar surface is not characterized by just a few giant convection cells.

3. Observed versus synthetic line profiles

We have used a 3D model to calculate the time variations for a number of spectral lines. Here, we display the resulting profile variations for the Fe I λ 6219 line (see Figs. 1 & 2, and samples of spatially resolved lines in Figs. 7 to 11).

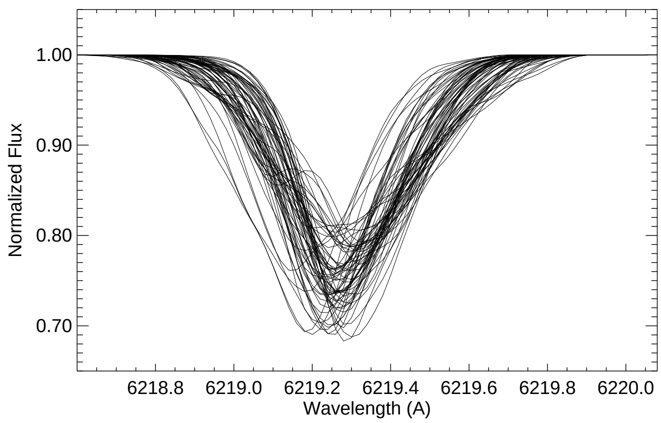

Figure 1. Variations in line profiles over 4.2 years of model time.

For this line, Gray (2000, Fig. 2) found line-depth variations of typically ±20% and a full width at half depth of about 25 km/s, varying between 23.5 km/s and 27 km/s over 17 months (with gaps resulting in about 11 months' effective coverage). However, the normalized line profile

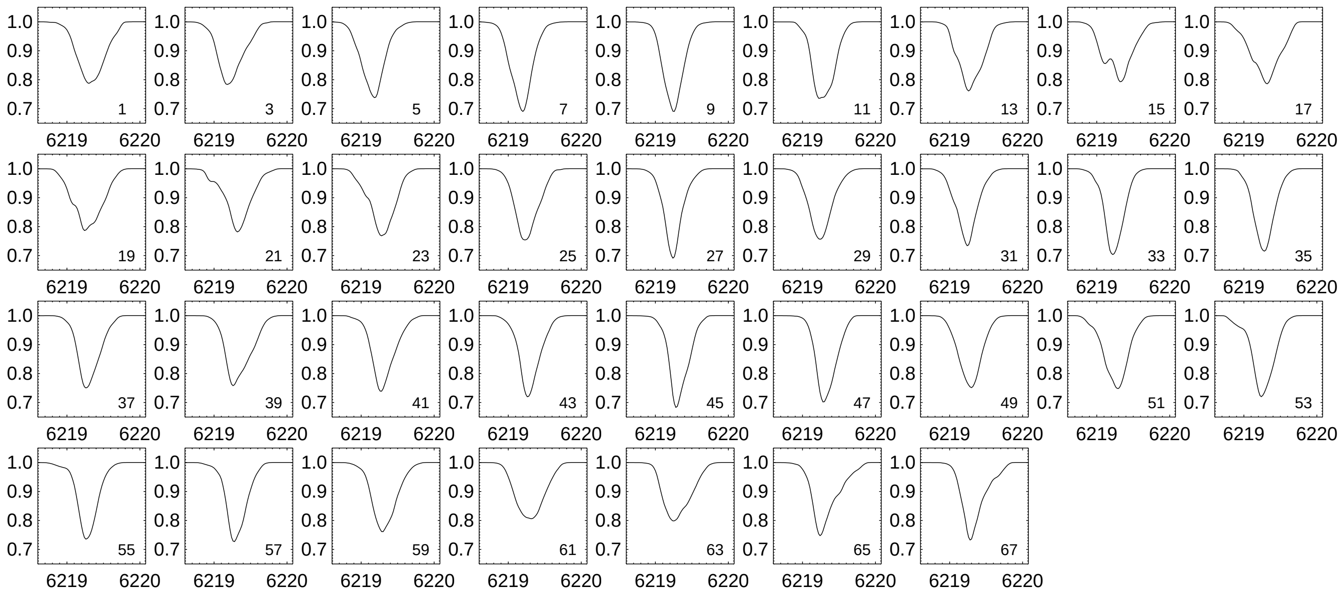

Figure 2. Variations in line profiles over 4.2 years of model time. Sample contributions to the disk-integrated spectrum shown in profile 35 are featured in Figs. 7 to 11.

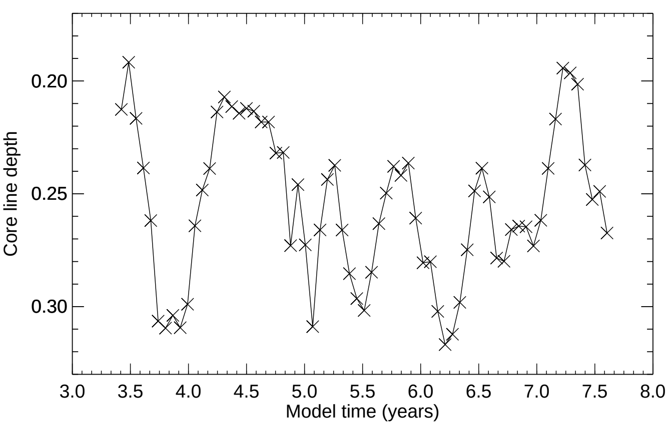

Figure 3. Variations in depth of line core over 4.2 years of model time.

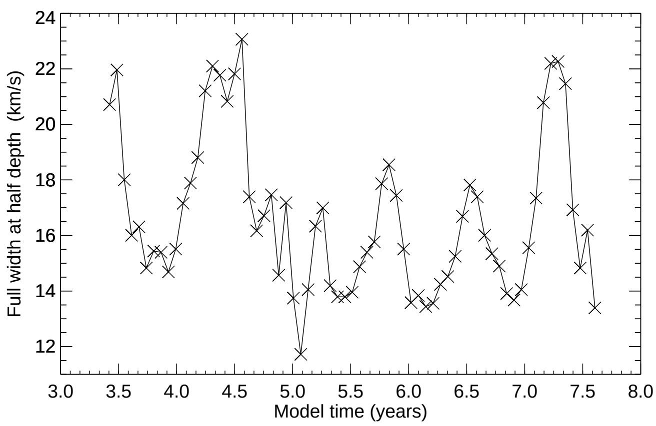

Figure 4. Variations in line width over 4.2 years of model time.

variations were at most on the order of 2% in rest intensity (Gray 2001, Fig. 6), which was interpreted as an "additional blend" and not as temporary bumps in profiles that resulted from giant convection cells.

The variations in the core line depths of our calculated profiles (Fig. 3) are similar to those found by Gray; however, the variations in half-width (Fig. 4) are significantly greater than those observed by Gray: the full width at half line depth varies by almost a factor of two, from 12 km/s to 23 km/s over 4 years, with an average of about 17 km/s. The reason is that the line profiles of the simulations (Figs. 1 & 2) show systematically much larger variations than those of the observed ones.

However, the 11 (or even 17) months of Gray's observations are not sufficient to derive precise results about the statistics of profile variations of Betelgeuse. For example, in the plot of the variations in the half-width of the synthetic lines (Fig. 4), it is easily possible to find a window of 17 months that has a smaller amplitude (in km/s) than the observed ones.

The smoothness of the synthetic profiles agrees well with the observations in Gray (2001). There is no trace of the fine-structured cores found in earlier observations (Gray 2000).

4. Conclusions

Taking into account the instrumental profile (with a resolution of about 3 km/s in Gray's observations) and especially the broadening of lines by blends in the spectrum synthesis would reduce the amplitude of the half-width variations somewhat and move the mean value closer to

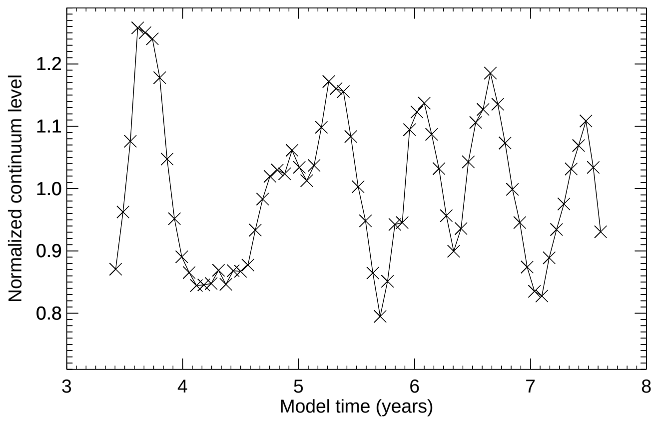

Figure 5. Variations in continuum level over 4.2 years of model time.

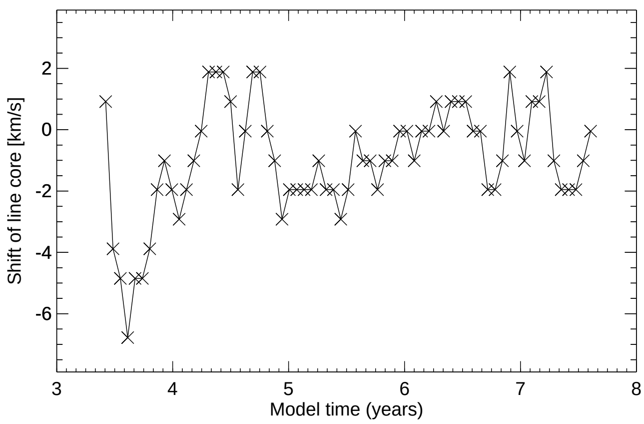

Figure 6. Variations in position of line core over 4.2 years of model time (from wavelength at minimum flux).

the observed one. However, the variations would still be larger than in the observations.

Although the simulated line profiles may still be plagued by a lack of spatial resolution in the radiative transfer and hydrodynamics as well as by the assumption of LTE, our results support the conclusion that the number of convective elements on Betelgeuse is greater than what is predicted by the present simulations. Before firm conclusions may be drawn, however, a more adequate mass (and thus greater gravity) must be adopted in the simulations. Also, the effects of shocks on the line profiles must be explored further, and the interferometric observations of large-scale departures from spherical symmetry and "bright spots" must be understood.

Extrapolating the results of the current $5\,M_\odot$ model to a (not yet extant) $10\,M_\odot$ model with the same radius would lead to about 4 times the number of surface cells and approximately half the amplitude of the variations. This simple (but computationally very demanding) adjustment of the model mass towards a more likely value for a red supergiant may bring simulations and observations into agreement—within the limits set by the complex behavior of Betelgeuse and the small time spans of data available.

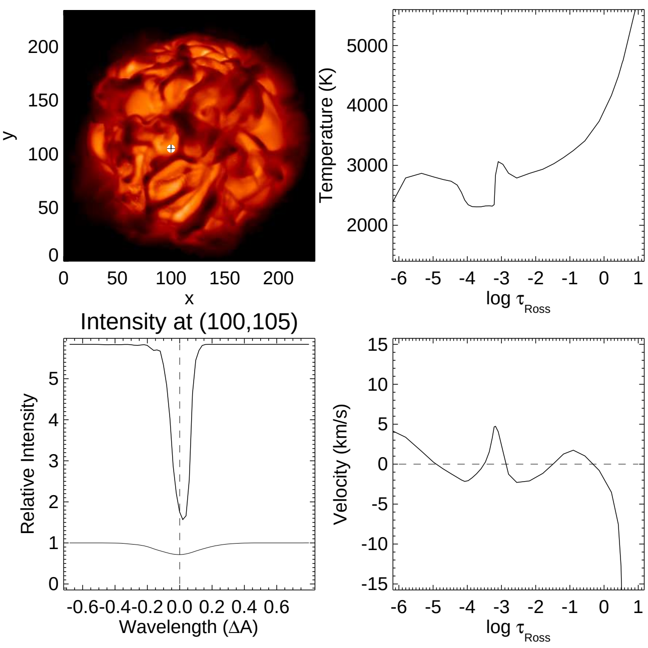

Figure 7. Sample line profile around 6219.281 Å. Upper left: continuum image with mark at the point from which the spectrum is taken. Upper right: temperature over logarithm of Rosseland optical depth. Lower left: thick line: sample spectrum vs. wavelength shift relative to λ=6219.281 Å; thin line: disk integrated spectrum with continuum normalized to one. Lower right: velocity along line of sight. This narrow profile is taken from a bright granule where the stratification shows rather small velocity fluctuations.

References

Burns, D., Baldwin, J. E., Boysen, R. C., et al. 1997, MNRAS 290, L11

Buscher, D. F., Baldwin, J. E., Warner, P. J., Haniff, C. A. 1990, MNRAS 245, 7P

Freytag, B., Steffen, M., Dorch, B. 2002, Astron. Nachr. 323, 213

Gilliland, L., Dupree, A. K. 1996, ApJ 463, L29

Gray, D. F. 2000, ApJ 532, 487

Gray, D. F. 2001, PASP 113, 1378

Lim, J., Carilli, C. L., White, S. M., et al. 1998, Nature 392, 575

Goldberg, L. 1984, PASP 96, 366

Schwarzschild, M. 1975, ApJ 195, 137

Young, J. S., Baldwin, J. E., Boysen, R. C., et al. 2000, MNRAS 315, 635

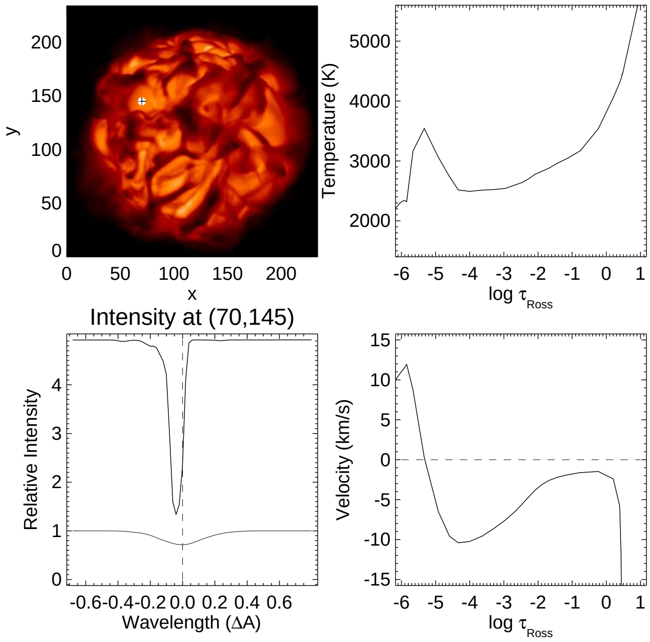

Figure 8. Sample line profile (see explanation in Fig. 7). A "granule profile" with a net blueshift.

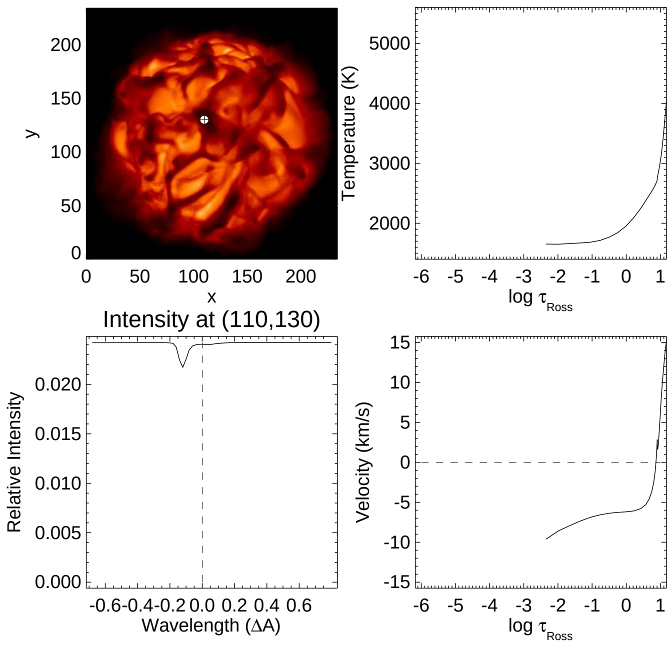

Figure 9. Sample line profile (see explanation in Fig. 7). Profile taken from a dark region with intensity ∼ 50 times lower than the "granule intensity."

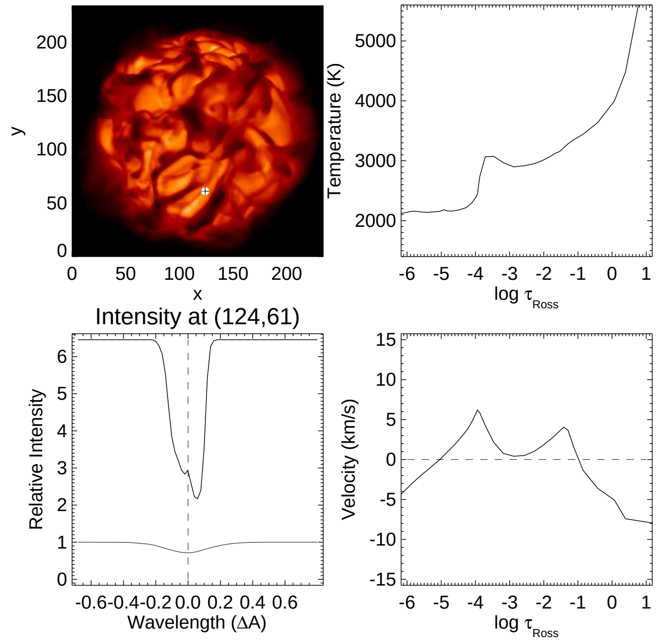

Figure 10. Sample line profile (see explanation in Fig. 7). A bright area with a double-bump profile.

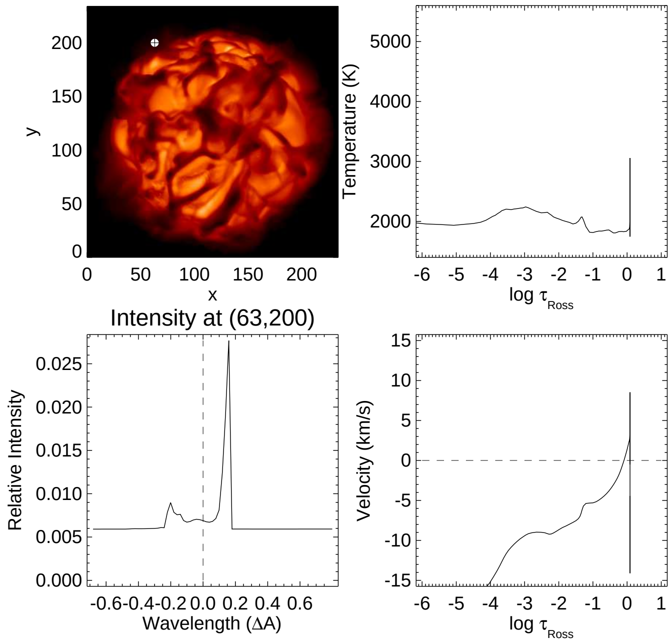

Figure 11. Sample line profile (see explanation in Fig. 7). Emission line from the limb. The entire Rosseland optical thickness of that column is just above one. The "spike" near $\tau_{\mathrm{Ross}} = 1$ is resolved on the model grid and has a finer structure than can be seen on the scale of the plots above.